Int J Clin Exp Pathol 2015;8(4):3460-3468
www.ijcep.com /ISSN:1936-2625/IJCEP0006250

Original Article

An enterovirus 71 strain causes skeletal muscle damage in infected mice

Peixin Lin[1], Lulu Gao[1], Yeen Huang[1], Qing Chen[2], Hong Shen[1]

[1]Department of Pathology, School of Basic Medical Sciences, Southern Medical University, Tonghe, Guangzhou, China; [2]Department of Epidemiology, School of Public Health and Tropical Medicine, Southern Medical University, Tonghe, Guangzhou, China

Received January 22, 2015; Accepted March 21, 2015; Epub April 1, 2015; Published April 15, 2015

Abstract: Objective: To study the target organs for enterovirus 71 (EV71) in infected suckling mice. Methods: 5-day-old BALB/c suckling mice were infected with an EV71 strain. Tissues of the infected mice were processed for histopathological examination, including immunohistochemistry, in situ hybridization, ultrastructural observation. Results: Some mice developed limb paralysis, trouble walking and loss of balance. Results of the histopathological study showed that a large amount of EV71 existed in the skeletal muscle tissues, accounting for the damage of the skeletal muscles. Conclusion: The EV71 clinical isolate used in this study presented evident myotropism. Skeletal muscles are important target organs for EV71 in the infected suckling mice. To clarify the relationship between EV71 infection and muscle diseases may contribute to a better understanding of the pathogenesis of EV71.

Keywords: Enterovirus 71, BALB/c mice, histopathological examination, skeletal muscle damage, myotropism, mitochondrial injury

Introduction

Enterovirus 71 (EV71) is a single-positive-stranded RNA virus, belonging to the Picornaviridae family. Since it was first identified in 1969, it has caused several large epidemics worldwide and countries in the Asia-Pacific region have experienced increased occurrence of EV71 infection in recent years [1]. EV71 infection mainly causes mild hand, foot and mouth disease (HFMD) and herpangina in infants and children under 6 years old, but may develop neurological diseases manifesting aseptic meningitis, encephalitis or poliomyelitis-like acute flaccid paralysis [2]. For the high rate of disability and lethality in severe EV71 infected patients, EV71 has been considered as the most important neurotropic enterovirus after the eradication of poliomyelitis and has posed a great threat to public health. However, the pathogenesis of EV71 infection remained to be clarified. Specific antiviral agent and vaccine have not been approved for clinical usage [3-5]. In view of the potential lethality and deficiency of effective treatment, researches regarding EV71 emerge in large numbers, such as the molecular epidemiology and evolution of EV71 strains, virulence determinants of the EV71 genome, the interaction between virus and host, the sensitive and practical experimental model and so on [6-10]. In our study, we used an EV71 strain to infect the 5-day-old BALB/c suckling mice and studied the target organs for EV71 by histopathological examination, which laid the foundation for the study of the pathogenesis of EV71.

Methods

Mice

Four cages of 5-day-old BALB/c suckling mice were used as the experimental subjects. Each cage has a minimum of six mice. All mice were obtained from the specific-pathogen-free facility of experimental animals' center of Southern Medical University. All animal experiments were performed according to animal care and welfare protocols.

Cell culture and virus

Vero cell lines were maintained in Dulbecco's modified Eagle's medium (DMEM) containing

10% fetal bovine serum (FBS). The EV71 isolate was obtained from the Department of Epidemiology, School of Public Health and Tropical Medicine, Southern Medical University, Guangzhou, China. This EV71 isolate was derived from an 8-month-old female infant with the fatal enterovirus 71 infection. After propagating in the Vero cell line and freezing and thawing three times, virus stocks were collected and stored at -80°C. The isolate has been identified as the human enterovirus type 71, belonging to Cluster C4, basically similar to the epidemic genotype in mainland China and neighboring countries [4].

Virus titration

The isolated virus was titrated in the Vero cells. Cells were cultured in DMEM supplemented with 10% FBS in 96-well cell culture microtitre plates. The growth medium was decanted and 100 μl virus stocks serially diluted in DMEM from 10^{-1}~10^{-10} was added and incubated at 37°C for 1 hour for adsorption. DMEM without virus was added as negative control. Maintenance medium containing 2% FBS was then added after decanting the virus stocks. The cells were incubated at 37°C in CO_2 atmosphere then. The wells were observed daily under inverted microscope for cytopathic effect (CPE), with the final reading made after 7 days. The end point titer was calculated in tissue culture infective dose 50 ($TCID_{50}$) per mL as described by Reed and Muench [11].

Animal infection experiment

In each cage, suckling mice were divided randomly into the experimental group which were injected intraperitoneally with 0.2 mL EV71 stocks in three consecutive days and the control group which were mock-infected with PBS. Mice were observed daily for signs of infection. Mice that showed paralysis, weakness and death were killed in time. Others were monitored up to 10 days and killed then. Tissue samples from the killed animals, including heart, lungs, liver, stomach, intestine, kidneys, cerebrum, cerebellum, brainstem, spinal cord, diaphragm and muscles, were collected and fixed in 10% neutral-buffered formalin.

Histological observation by light microscopy

After fixation, dehydration of gradient ethanol and xylene transparent, tissue samples were embedded in paraffin. 2-μm-thick paraffin-embedded tissue sections were placed onto siliconized slides and stained with hematoxylin and eosin. The histopathology of each tissue sample was observed under light microscopy.

Immunohistochemical staining

For virus staining, tissue sections were dewaxed, dehydrated and antigen repaired by pressure cooker method in the sodium citrate solution. Then the sections were incubated with 3% H_2O_2 (15 min), MOM mouse immunoglobulin G blocking reagent (Vector Laboratories, Burlingame, CA) (1 h), anti-EV71 monoclonal antibody (MAb) (1:2000 dilution, Millipore) (30 minutes), and biotinylated anti-mouse IgG (10 minutes). Streptavidin-based detection system was applied afterwards. The sections were observed with a light microscope after counterstaining. Control sections were incubated with PBS instead of MAb in order to check for the absence of a non-specific effect due to the secondary antibody (biotinylated anti-mouse IgG).

In situ hybridization

Digoxigenin (DIG) labeled cRNA probes were prepared for in situ hybridization. The probes were composed of approximately 500-bp nucleotides generated from a reverse transcriptase polymerase chain reaction (RT-PCR) procedure and published primers [12] to the 5-nontranslated region of EV71. Then the PCR fragments were cloned into pBluescript II SK(-) with XhoI and EcoRI enzyme restriction site and transferred into DH5a. The cRNA probe was synthesized with Roche DIG RNA Labeling Kit (Life Technologies).

Limbs of EV71 infected mice were fixed overnight in 4% paraformaldehyde at 4°C and embedded in paraffin. 5-μm-thick tissue sections were processed for in situ hybridization. The tissue slides were dewaxed, dehydrated, and digested with 100 μg/mL proteinase K at 37°C for 20 minutes. The sections were then prehybridized at 70°C for 2 hours before hybridized at 70°C overnight. After hybridization, slides were washed in 4×, 2×, 1×, 0.5× saline sodium citrate at 37°C respectively. Hybridization was detected by anti-DIG Fab fragments linked to alkaline phosphatase and a color reaction was obtained when nitroblue tetrazolium/5-bromo-4-chloro-3-indolyl phosphate (NBT/BCIP) was applied.

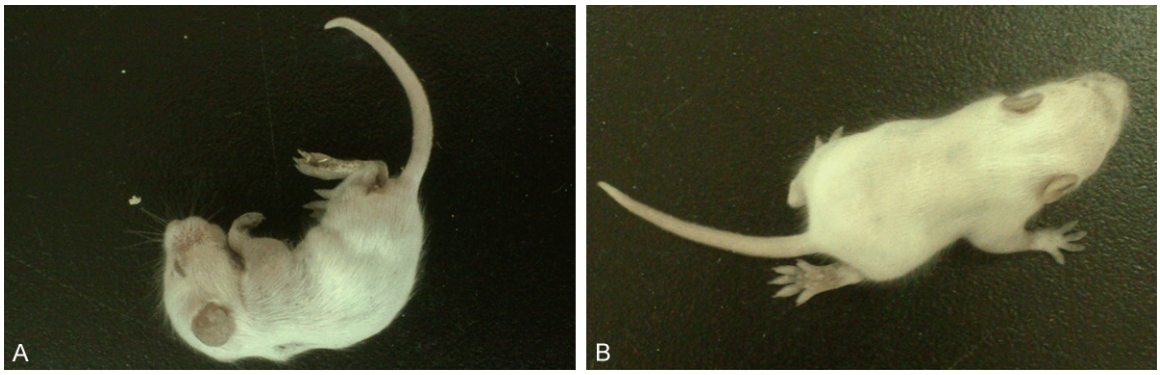

Figure 1. Clinical sign of the EV71 infected mice. Some infected mice developed weakness and drooping after infection of EV71 (A). Some manifested limb paralysis, trouble walking and loss of balance after day 5 post-infection (B).

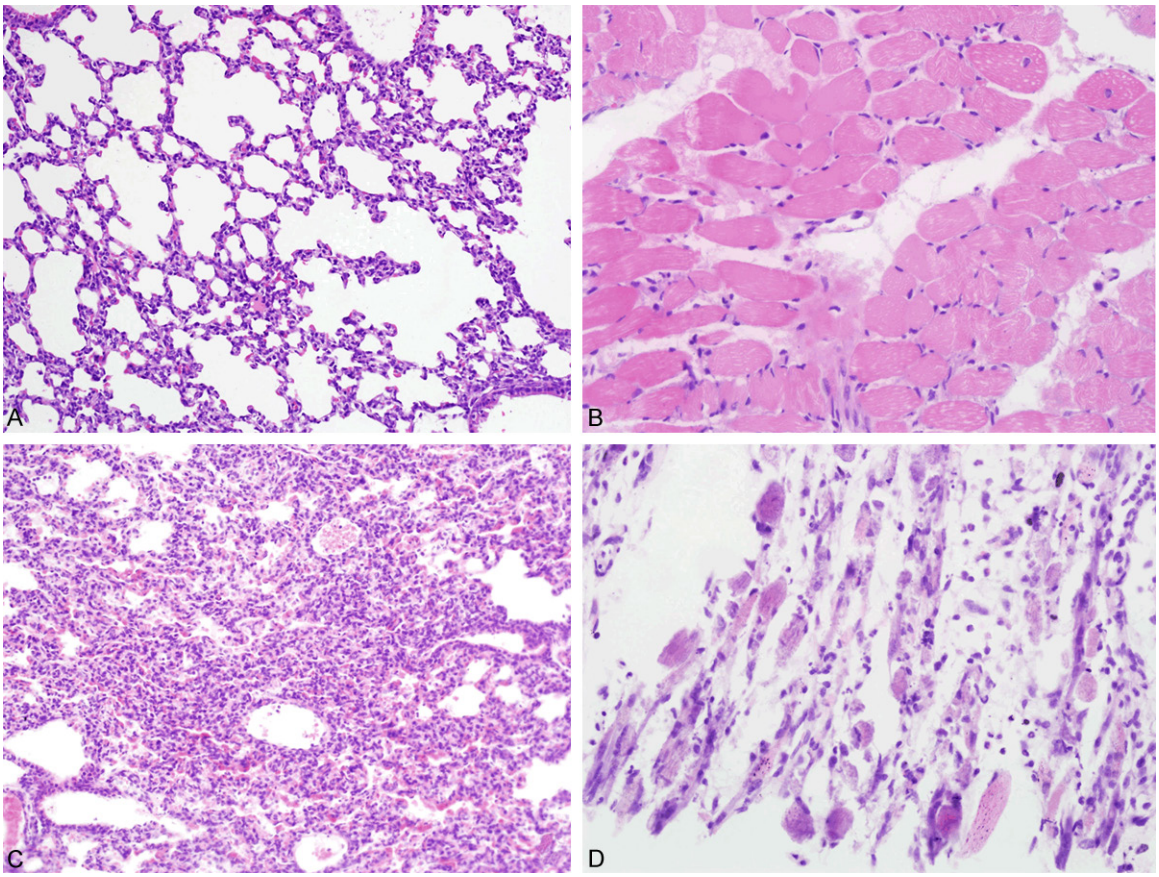

Figure 2. Histological features of tissues of the infected mice-1. Pictures in the top row showed normal histological features of the lungs (A) and skeletal muscles (B) of mice in the control group. In EV71 infected mice, obvious inflammatory cells exudation was observed in alveolar spaces of lung tissues (C). The skeletal muscle tissues of the limbs presented myofibril fracture and myocyte disruption (D).

Electron microscopy

Small pieces (1 mm^3) of the skeletal muscle tissues of the paralyzed limbs from the infected mice were fixed in 4% glutaraldehyde for at least 2 hours in 4°C and washed 3 times in the phosphate buffer (pH 7.0) before postfixation in 1% osmium tetroxide for 1 hour. The tissues were then washed 3 times in the phosphate buffer and dehydrated by a graded series of ethanol. After infiltrated with absolute acetone and the mixture of absolute acetone and the

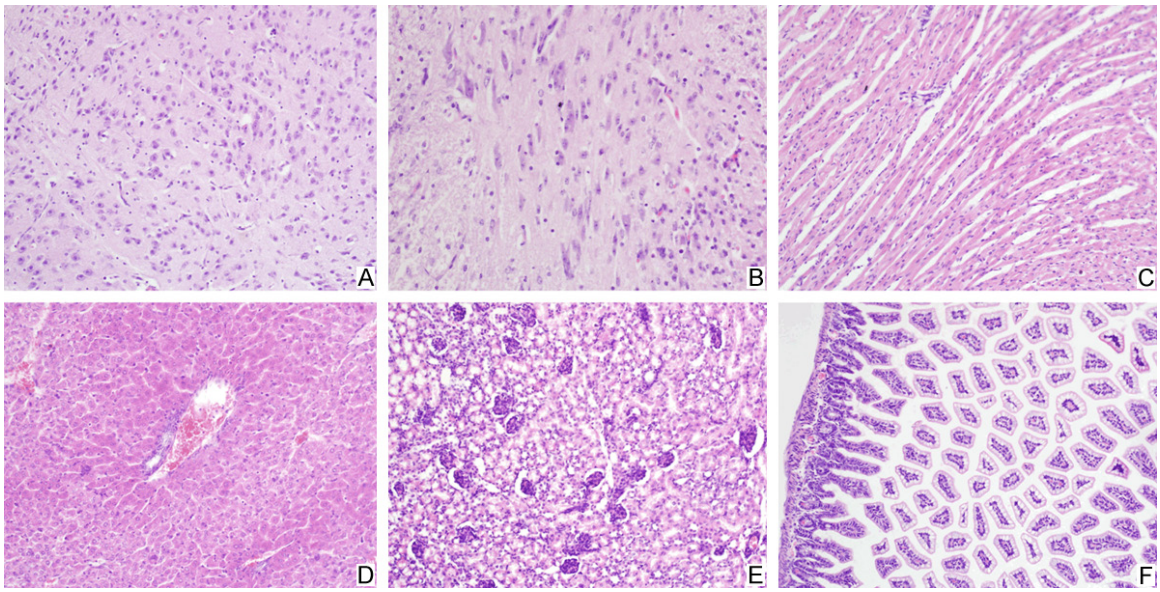

Figure 3. Histological features of tissues of the infected mice-2. In EV71 infected mice, mild inflammatory cells infiltration was presented in the tissues of the cerebrum (A) and the spinal cord (B). The cardiac myocytes were intact without disruption (C). No pathological changes were observed in tissues of the liver (D), the kidney (E) and the intestine (F).

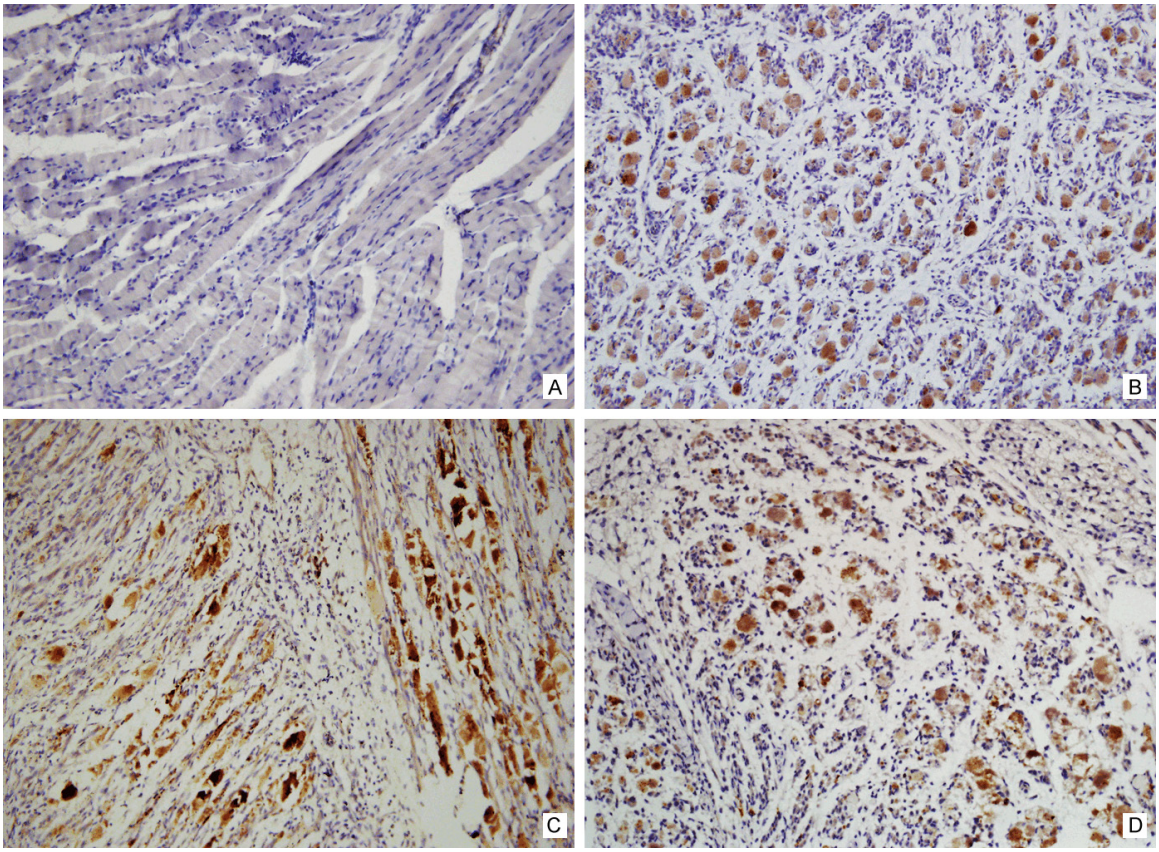

Figure 4. Detection of VP1 protein of EV71 by immunohistochemistry method-1. Immunohistochemistry staining of the skeletal muscle tissues of the normal mice was as negative control (A). By contrast, the evident staining was exhibited in skeletal muscles of the EV71 infected mice, including the limbs (B), the intercostal spaces (C) and even along the spine (D).

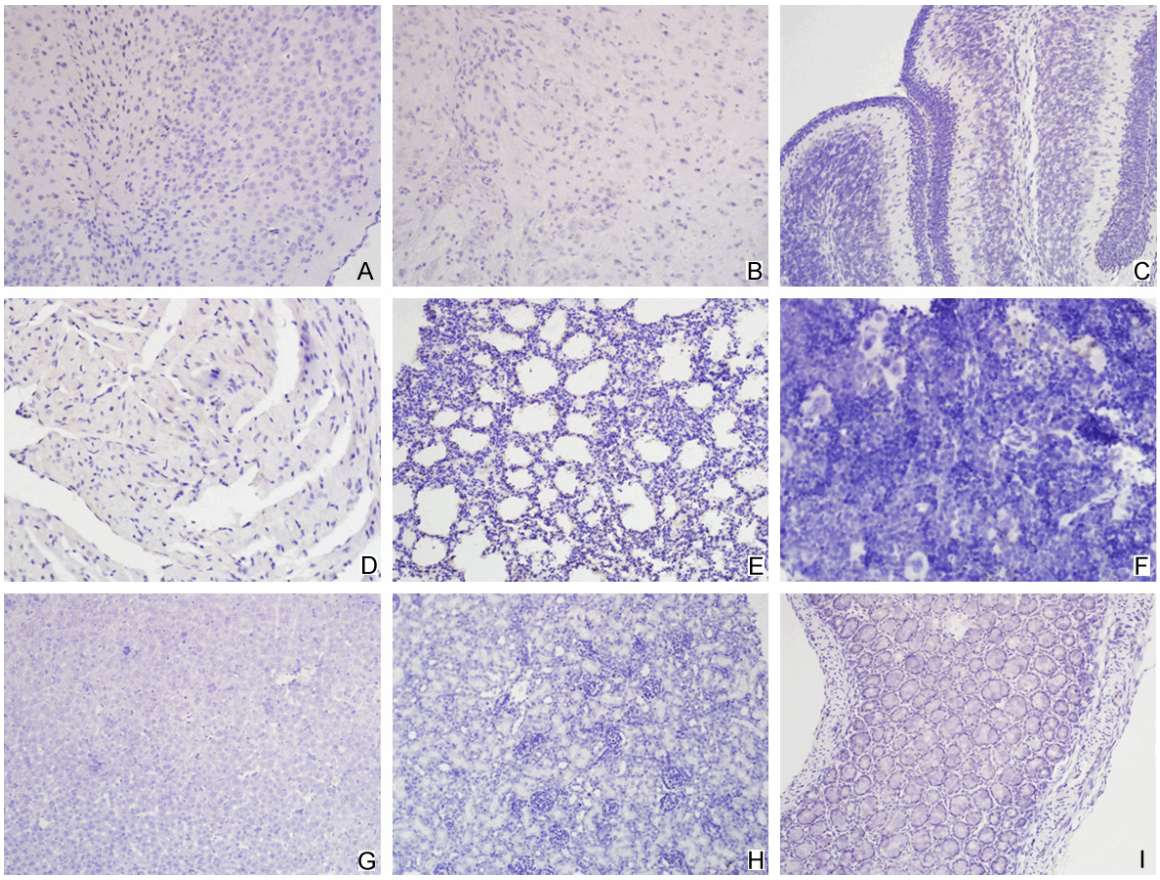

Figure 5. Detection of VP1 protein of EV71 by immunohistochemistry method-2. Tissues of the cerebrum (A), brainstem (B), cerebellum (C), heart (D), lung (E), spleen (F), liver (G), kidney (H) and intestine (I) displayed negative staining.

final Spurr resin mixture, the tissues were placed in capsules containing embedding medium and heated at 70°C overnight. Selected 60 nm to 80 nm ultrathin sections were collected on copper grids and stained with uranyl acetate and lead citrate before observing in transmission electron microscopy.

Result

A murine model of enterovirus 71 infection

$TCID_{50}$ of the EV71 strain used in this experiment was $10^{-5.81}$/0.1 mL, indicating that 50% cultured cells processed with $10^{5.81}$-fold-diluted virus stocks presented cytopathic effect. After infection with 0.2 mL virus stocks per day for three consecutive days (the experimental group) and an equal amount of PBS (the control group), clinical sign of the mice was noted. Compared with the control group, EV71 infected mice had poor reacting ability. The hair was sparse and lackluster and the body weight increased slowly. Some infected mice developed obvious limb paralysis, trouble walking and loss of balance after day 5 post-infection (**Figure 1**).

Pathological observation of the infected mice

Histologically, lung tissues showed inflammatory cells exudation in alveolar spaces. Myofibril fracture and myocyte disruption were found in the muscle tissues of the limbs, the intercostal spaces and even along the spine (**Figure 2**). Tissues of the cerebrum and the spinal cord presented mild inflammatory cells infiltration, but no injury of the brain parenchyma was found. No pathological changes were observed in other tissues (**Figure 3**).

On immunohistochemistry, anti-VP1 antibody was applied to detect the VP1 protein of EV71. Skeletal muscle tissues exhibited the positive staining, indicating vigorous virus replication

Human enterovirus 71 strain 57-ZZ-HN-CHN-2010 5' UTR
Sequence ID: gb|JF732907.1| Length: 743 Number of Matches: 1

Range 1: 66 to 565 GenBank Graphics ▼ Next Match ▲ Previous Match

Score	Expect	Identities	Gaps	Strand
876 bits(474)	0.0	495/504(98%)	6/504(1%)	Plus/Minus

```
Query  1    GAAACACGGACACCCAAAGTAGTCGGTTCCGCTGCAGAGTTACCCGTTACGACACACTAC  60
            ||||||||||||||||||||||||||||||||||||||||||||||||||||||||||||
Sbjct  565  GAAACACGGACACCCAAAGTAGTCGGTTCCGCTGCAGAGTTACCCGTTACGACACACTAC  506

Query  61   CCGCTGGCTTGTGGGCGTGTGCTCCGCAGTTGGGATTAGCCGCATTCAGGGGCCGGAGGA  120
            ||||||||||||||||||||||||||||||||||||||||||||||||||||||||||||
Sbjct  505  CCGCTGGCTTGTGGGCGTGTGCTCCGCAGTTGGGATTAGCCGCATTCAGGGGCCGGAGGA  446

Query  121  CTACTAACTAGCTCAGTAGACTCTTCACACCATGTCCGTATTAGAGCGCCCCATGGGTTA  180
            ||||||||||||||||||||||||||||||||||||||||||||||||||||||||||||
Sbjct  445  CTACTAACTAGCTCAGTAGACTCTTCACACCATGTCCGTATTAGAGCGCCCCATGGGTTA  386

Query  181  CCCCATGGGCAGGCCGCCAACGCAGCCACCGCCACGGTCGCCCGTGGGGAATGCGGTGAC  240
            ||||||||||||||||||||||||||||||||||||||||||||||||||||||||||||
Sbjct  385  CCCCATGGGCAGGCCGCCAACGCAGCCACCGCCACGGTCGCCCGTGGGGAATGCGGTGAC  326

Query  241  TCATCGACCTGATCTACACTGGGGGAGTGCTGAGCGAAGCTCTCCGCAACTTTCATGGTG  300
            |||||||||||||||||||||||||||||| ||||||||||||||||||||||||||||
Sbjct  325  TCATCGACCTGATCTACACTGGGGGAGTGCTGAACGAAGCTCTCCGCAACTTTCATGGTG  266

Query  301  TTACTAGGTTTTCCGAAGTAGCTAGCCGGATAACGAACGTTTTCTCCTTCAACCGCGCGA  360
            ||||||||||||||||||||||||||||||||||||||||||||||||||||||||||||
Sbjct  265  TTACTAGGTTTTCCGAAGTAGCTAGCCGGATAACGAACGTTTTCTCCTTCAACCGCGCGA  206

Query  361  GCAGTCTATTGATACTCAGTCCGGGGAAACAGAAGTGCTTGATCAAGACATAACTGGAGC  420
            ||||||||||||||||||||||||||||||||||||||||||||||||||||||||||||
Sbjct  205  GCAGTCTATTGATACTCAGTCCGGGGAAACAGAAGTGCTTGATCAAGACATAACTGGAGC  146

Query  421  GTTATGCCTGCTATTGATCGTGGTTTGCTGCTTCTAAGTTTCACTggggggggggTGTA-A  479
            |||||||| ||||||||||||||||||||||||||||||||||||||||||| ||| |
Sbjct  145  GTTATGCCCGCTATTGATCGTGGTTTGCTGCTTCTAAGTTTCACTGGGGGGGGGGGGTATA  86

Query  480  AA-CATGGCGTCACAAGAGTGTAC  502
            || || |||| ||||| || ||||
Sbjct  85   AAACA-GGCG-CACAA-AG-GTAC  66
```

Figure 6. The gene sequencing and BLASTn results of the detected EV71 gene fragment. The genetic sequence of the detected EV71 gene fragment was similar to the published 5-nontranslated region of the EV71 genome.

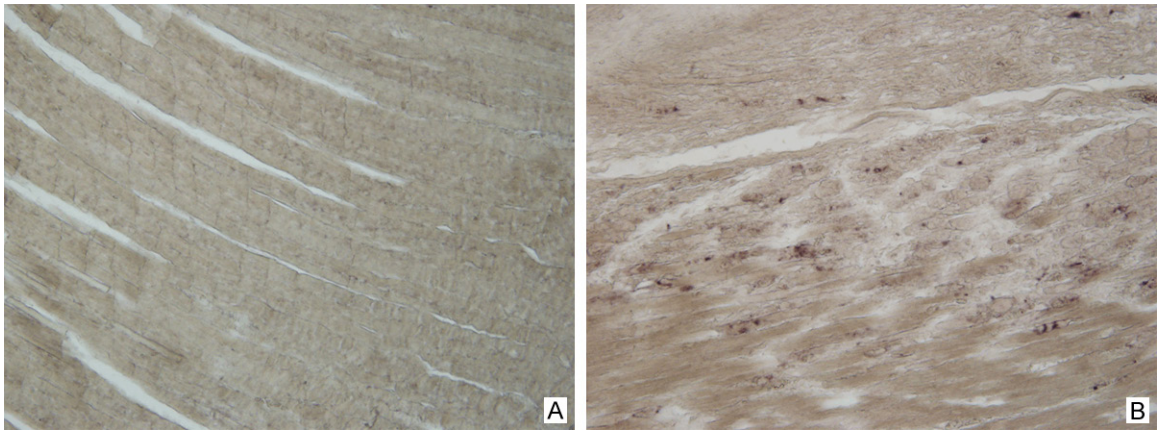

Figure 7. Detection of nucleic acid of EV71 by in situ hybridization method. The skeletal muscle tissues of the normal mice were as negative control (A). Positive staining was seen in the skeletal muscle tissues of the paralyzed limbs of the infected mice (B).

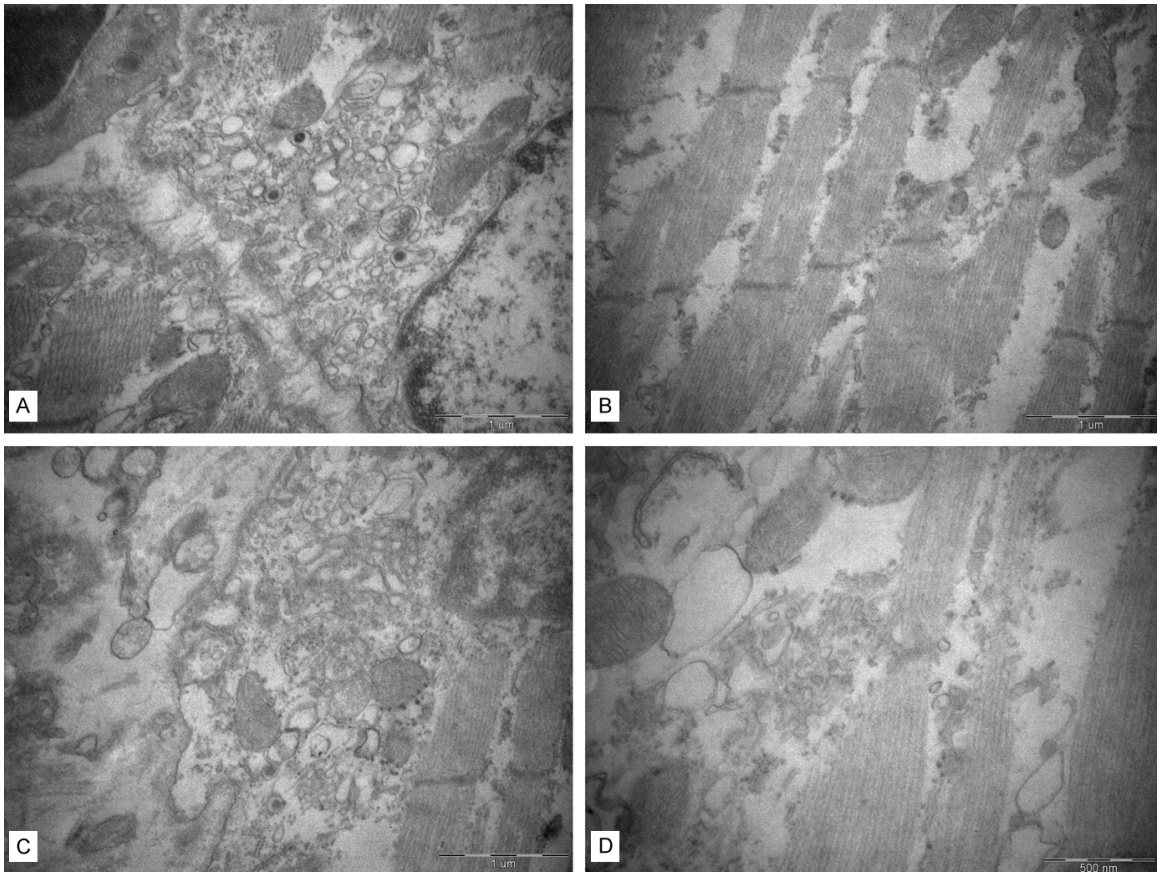

Figure 8. The ultrastructure of the skeletal muscle of the paralyzed limb. Obvious myofibril disorder and fracture were seen. Damaged mitochondria presented swelling, vacuole and degeneration.

(**Figure 4**). Other organs displayed negative staining (**Figure 5**).

For in situ hybridization, prepared probes were used to detect the 5-nontranslated region of the EV71 genome, which had been identified by gene sequencing and BLASTn (**Figure 6**). Positive staining was seen in the skeletal muscle tissues of the paralyzed limbs of the infected mice, paralleling to the immunohistochemical findings (**Figure 7**).

The skeletal muscle tissues of the paralyzed limb were harvested for ultrastructural observation. Obvious myofibril disorder and fracture were seen. Most of the mitochondria presented swelling, vacuole and degeneration. These ultrastructural changes showed strong evidence of the skeletal muscle damage (**Figure 8**).

Discussion

Severe EV71 infection mainly manifests neurological complication and cardiopulmonary dysfunction clinically. So EV71 is considered as one of the most important neurotropic virus. For studying the pathogenesis of EV71-induced diseases, animal models with nervous system involvement have been generated [13], like human SCARB2 transgenic mice model [9] and mouse-adapted EV71 strain infected mice model [14]. In our study, we used an EV71 clinical strain to infect the BALB/c suckling mice and study the target organs for EV71. EV71 infected mice manifested general weakness compared to the control group, and some developed obvious limb paralysis. The histopathological examination discovered significant pathological changes in the skeletal muscle tissues of the infected mice. Although evident viral particles were not found by light microscopy and transmission electron microscopy, the result of immunohistochemistry and in situ hybridization proved that a large amount of EV71 existed in the skeletal muscle tissues, accounting for the damage of the skeletal muscle. The lung, the cerebrum and the spinal cord showed inflammatory cells infiltration, but no

positive EV71 antigen was detected in these tissues. These results proved that besides neurotropism, EV71 also exhibits strong myotropism in mice. Some researchers had reported that skeletal muscle tissues had evident tropism and susceptibility to EV71 in infected mice models. The diseased mice had much more virus in their muscles than in brains [15]. But in humans, the skeletal muscle tissues were negative for EV71 antigen [16]. Some previous studies demonstrated that the distribution features of the virus in the skeletal muscle, the spinal cord and the brain of the infected mice indicated that the virus may enter the nervous system via peripheral motor nervous route after skeletal infection [17, 18]. Evident damage of nervous system was not found in our study, which might be related to the viral dose, the route of infection, the immune ability of the host, the tropism of the virus strain and so on. The mechanism of the neurotropism and myotropism in EV71 infected mice is still an issue that needs further study.

Scavenger receptor class B, member 2 (SCARB2) is located in limiting membranes of lysosomes and endosomes, and may participate in membrane transportation and the reorganization of endosomal/lysosomal compartment. There is increasing evidence that SCARB2 functions as a receptor for EV71 in human [19]. But a previous study demonstrated that there was no clear correlation between mouse SCARB2 and EV71 antigen distribution in the infected mice [16]. A specific receptor for EV71 in mice remains to be identified.

Mitochondria are the main power-generating and free-radical-clearing organelles. Dysfunction of the mitochondria may disrupt the cellular homeostasis and induce apoptosis. Mitochondrial injury in the process of viral infection has aroused general attention in the recent years [20]. In our study, the ultrastructure of the damaged skeletal muscle tissues showed prominent mitochondrial injury. It implied that EV71 may cause the damage of the skeletal muscle tissues via a mitochondria-dependent pathway.

Therefore, we propose questions what factors may determine the EV71 tropism, what pathogenic mechanisms may be involved in the skeletal muscle damage and when EV71 may enter the nervous system by retrograde axonal transportation after muscle infection. In our view, clarifying the unknown cause of the skeletal muscle damage in the infected mice may be of value in the study of the pathogenesis of EV71 and even muscle diseases [21].

Acknowledgements

These works were supported by Specialized Research Fund for the Doctoral Program of Higher Education (K1014090) and Guangdong Natural Science Foundation (S2011040003-732, S2012010009540).

Disclosure of conflict of interest

None.

Address correspondence to: Hong Shen, Department of Pathology, School of Basic Medical Sciences, Southern Medical University, Tonghe, Guangzhou, China. Tel: +8613580569099; E-mail: shenhong2010168@163.com

References

[1] McMinn PC. An overview of the evolution of enterovirus 71 and its clinical and public health significance. FEMS Microbiol Rev 2002; 26: 91-107.

[2] Huang CC, Liu CC, Chang YC, Chen CY, Wang ST and Yeh TF. Neurologic complications in children with enterovirus 71 infection. N Engl J Med 1999; 341: 936-942.

[3] Wu KX, Ng MM and Chu JJ. Developments towards antiviral therapies against enterovirus 71. Drug Discov Today 2010; 15: 1041-1051.

[4] Solomon T, Lewthwaite P, Perera D, Cardosa MJ, McMinn P and Ooi MH. Virology, epidemiology, pathogenesis, and control of enterovirus 71. Lancet Infect Dis 2010; 10: 778-790.

[5] Zhang D, Lu J and Lu J. Enterovirus 71 vaccine: close but still far. Int J Infect Dis 2010; 14: e739-743.

[6] Shih SR, Stollar V and Li ML. Host factors in enterovirus 71 replication. J Virol 2011; 85: 9658-9666.

[7] Huang HI, Weng KF and Shih SR. Viral and host factors that contribute to pathogenicity of enterovirus 71. Future Microbiol 2012; 7: 467-479.

[8] Brown BA, Oberste MS, Alexander JP Jr, Kennett ML and Pallansch MA. Molecular epidemiology and evolution of enterovirus 71 strains isolated from 1970 to 1998. J Virol 1999; 73: 9969-9975.

[9] Lin YW, Yu SL, Shao HY, Lin HY, Liu CC, Hsiao KN, Chitra E, Tsou YL, Chang HW, Sia C, Chong

P and Chow YH. Human SCARB2 transgenic mice as an infectious animal model for enterovirus 71. PLoS One 2013; 8: e57591.
[10] Singh S, Poh CL and Chow VT. Complete sequence analyses of enterovirus 71 strains from fatal and non-fatal cases of the hand, foot and mouth disease outbreak in Singapore (2000). Microbiol Immunol 2002; 46: 801-808.
[11] Reed LJ and Munch H. A simple method of estimating fifty percent endpoints. Am J Hyg 1938; 7: 493-497.
[12] Arola A, Kalimo H, Ruuskanen O and Hyypiä T. Experimental myocarditis induced by two different coxsackievirus B3 variants: aspects of pathogenesis and comparison of diagnostic methods. J Med Virol 1995; 47: 251-259.
[13] Chen YC. A murine oral enterovirus 71 infection model with central nervous system involvement. J Gen Virol 2004; 85: 69-77.
[14] Wang YF, Chou CT, Lei HY, Liu CC, Wang SM, Yan JJ, Su IJ, Wang JR, Yeh TM, Chen SH and Yu CK. A mouse-adapted enterovirus 71 strain causes neurological disease in mice after oral infection. J Virol 2004; 78: 7916-7924.
[15] Chumakov M, Voroshilova M, Shindarov L, Lavrova I, Gracheva L, Koroleva G, Vasilenko S, Brodvarova I, Nikolova M, Gyurova S, Gacheva M, Mitov G, Ninov N, Tsylka E, Robinson I, Frolova M, Bashkirtsev V, Martiyanova L and Rodin V. Enterovirus 71 isolated from cases of epidemic poliomyelitis-like disease in Bulgaria. Arch Virol 1979; 60: 329-340.
[16] Yu P, Gao Z, Zong Y, Bao L, Xu L, Deng W, Li F, Lv Q, Gao Z, Xu Y, Yao Y and Qin C. Histopathological features and distribution of EV71 antigens and SCARB2 in human fatal cases and a mouse model of enterovirus 71 infection. Virus Res 2014; 189: 121-132.
[17] Chen CS, Yao YC, Lin SC, Lee YP, Wang YF, Wang JR, Liu CC, Lei HY and Yu CK. Retrograde axonal transport: a major transmission route of enterovirus 71 in mice. J Virol 2007; 81: 8996-9003.
[18] Ong KC, Badmanathan M, Devi S, Leong KL, Cardosa MJ and Wong KT. Pathologic characterization of a murine model of human enterovirus 71 encephalomyelitis. J Neuropathol Exp Neurol 2008; 67: 532-542.
[19] Jiao XY, Guo L, Huang DY, Chang XL and Qiu QC. Distribution of EV71 receptors SCARB2 and PSGL-1 in human tissues. Virus Res 2014; 190: 40-52.
[20] Huttemann M, Lee I, Pecinova A, Pecina P, Przyklenk K and Doan JW. Regulation of oxidative phosphorylation, the mitochondrial membrane potential, and their role in human disease. J Bioenerg Biomembr 2008; 40: 445-456.
[21] Douche-Aourik F, Berlier W, Feasson L, Bourlet T, Harrath R, Omar S, Grattard F, Denis C and Pozzetto B. Detection of enterovirus in human skeletal muscle from patients with chronic inflammatory muscle disease or fibromyalgia and healthy subjects. J Med Virol 2003; 71: 540-547.